

## Formation of kinetically trapped gels in the maltodextrin–gelatin system

Stefan Aleviopoulos<sup>a</sup>, Stefan Kasapis<sup>a,\*</sup>, Rukmal Abeysekera<sup>b</sup>

<sup>a</sup> *Department of Food Research and Technology, Cranfield University, Silsoe College, Silsoe, Bedfordshire, MK45 4DT, UK*

<sup>b</sup> *Institute for Applied Biology, University of York, Yorkshire, YO1 5DD, UK*

Received 16 February 1996; accepted 21 June 1996

---

### Abstract

A simple experimental procedure of cooling mixed maltodextrin–gelatin systems at various scan rates and to a range of final temperatures was employed to determine whether the state of thermodynamic equilibrium in solution is sustained in the structural organisation of the composite gels. Small-deformation dynamic oscillation and visible spectrophotometry results demonstrate that the development of network rigidity and the polymeric weight ratio at which phase inversion occurs in the mixture is heavily governed by the applied thermal regime. There is an antagonistic effect operating between ordering–aggregation leading to gelation and the extent of phase separation, with rapid quenching and slow cooling (e.g., 1 °C/min) promoting the former and latter mechanism, respectively. Theoretical modelling indicates that either polymeric component holds disproportionate amounts of solvent in its phase when it forms the continuous matrix. It was concluded that, within the experimental time–temperature constraints, composite gels are kinetically trapped away from conditions of thermodynamic equilibrium observed for their mixtures in solution. © 1996 Elsevier Science Ltd.

*Keywords:* Maltodextrin; Gelatin; Phase separation; Kinetic effects; Solvent partition

---

### 1. Introduction

The late 60's saw the advent of research on the conformational characteristics and functional properties of aqueous polysaccharide solutions and gels. Thus, work on alternating, non-gelling segments of iota-carrageenan, using optical rotation and con-

---

\* Corresponding author.

trolled cooling, suggested a transition from disordered polysaccharide coils to ordered double helices [1]. This outcome in combination with X-ray diffraction studies allowed the calculation of values for the angles along the glycosidic linkages of a sterically feasible iota double helix [2], an approach which became immensely useful in the designing of conformational maps for the industrially important polysaccharides [3]. The interactions between cations and polyelectrolyte polysaccharides were also investigated, since at certain conditions of temperature and stoichiometric equivalence they result in the formation of a three-dimensional network. Among these models, the specific chelation of  $\text{Ca}^{2+}$  with polyguluronate blocks of alginate stands out, and it has been explained in terms of an 'egg-box' arrangement which involves arrays of site-bound calcium ions sandwiched between intermolecular polyguluronate segments in a two-fold conformation [4].

Having developed a good understanding of the conformation–function relationships in single polysaccharide systems, researchers in the 70's initiated a systematic study into biopolymer interactions and especially into the extent of thermodynamic incompatibility between proteins and polysaccharides in solution. For more than 30 mixtures, it was found that phase separation into two liquid layers can occur when the total polymer concentration exceeds 4%, depending, of course, on pH and ionic strength [5]. Thus, limited compatibility between proteins and ionic polysaccharides is observed when the pH value is higher than the isoionic point of the protein or, regardless of pH, the ionic strength is greater than 0.25 [6,7]. Each liquid layer was found to be rich in one polymer and depleted in the other, and vice versa, with both polymers having reached conditions of thermodynamic equilibrium in solution. The phase equilibria led to the construction of phase diagrams whose asymmetric shape reflects the molecular weight differences between, for example, a globular protein and a plant polysaccharide [8].

Until then, the structural properties of phase-separated biopolymer gels were monitored on a purely descriptive basis, mainly to serve in the development of new products which was done on a 'hit and miss' basis. In the early 80's, however, an attempt was made to predict and control the mechanical characteristics of the agar–gelatin composite gel from those of the individual components [9]. First a theoretical expression (cascade formalism) was employed to follow the development of storage modulus as a function of polymer concentration. The amount of solvent kept in each phase was crucial to the exercise, since it would determine the effective polymer concentration and hence the rigidity of a phase. Therefore, trial values of the relative partition of solvent between the two phases ( $p$  factor) were used in the Takayanagi 'blending laws' [10] until a reasonable fit with the experimental results was achieved. The overriding assumption in the agar–gelatin work was that phase separation to thermodynamic equilibrium takes place first in solution, with gelation, upon subsequent cooling, maintaining the phase equilibria in the composite.

Recently, the quantitative exploration of binary biopolymer preparations was revived, and work focused mainly on the gelatin–maltodextrin system which has been used widely for the development of novel products [11]. Mixed solutions were made by fixing the amount of gelatin and increasing the maltodextrin concentration. Preparations produce single-phased transparent solutions or, at higher concentrations of maltodextrin, develop turbidity and upon centrifugation resolve into two liquid layers at equilibrium

whose composition defines a phase diagram [12]. Quench-cooling of the clear solutions results in continuous gelatin gels which undergo an ongoing deswelling and solvent repartition due to ordering of the slower gelling maltodextrin component. Application of the same thermal regime to the micro phase-separated solutions yields composite gels with maltodextrin as the continuous phase supporting the discontinuous gelatin inclusions [13]. A single solvent partition value was calculated for this range of maltodextrin concentrations but it was difficult to say whether the gelatin and maltodextrin phases coexist in the gel state at thermodynamic equilibrium. This paper provides a systematic study of the kinetics of phase separation in maltodextrin–gelatin gels, in an attempt to promote scientific debate and to facilitate intelligent manipulation of product applications.

## 2. Experimental

*Materials.*—The gelatin sample of this investigation was kindly provided by Systems Bio-Industries, Research Centre, Baupte, F-50500 Carentan, France. It was the second extract obtained from ossein by the lime pretreatment process (LO-2), a high quality gelatin with a Bloom value of 270. The isoelectric point (*pI*) was obtained by completely deionising the sample on a bed of ion-exchange resin and measuring the pH of the eluent. The *pI* value was pH 5.02, thus producing a negatively charged gelatin sample at the neutral pH of our investigation. Gel permeation chromatography (GPC), calibrated with gelatin standards of known absolute mass distribution, yielded a number-average molecular weight of  $0.86 \times 10^5$  and a mass-average molecular weight of  $2.1 \times 10^5$  with the content of alpha, beta, and gamma chains, which is roughly proportional to the gel strength, being 29.3, 17.2 and 8.8%, respectively. The concentration dependence of storage modulus ( $G'$ ) was fitted in terms of the cascade model, yielding an equilibrium constant of  $179.2 \text{ mol l}^{-1}$ , a functionality of 10.2, a front factor of 2.5, and a minimum critical gelling concentration ( $C_o$ ) of 0.72% [14]. A very acceptable sum of minimised differences of  $[\log G'_{\text{cal}} - \log G'_{\text{exp}}]^2$  in the least-squares fit (0.012) allows prediction of the gel rigidity at any concentration of a gelatin gel.

The maltodextrin sample used was provided by Avebe, 9607 PT Foxhol, The Netherlands. It is a neutral dextrin produced enzymatically from potato starch and is commercially available under the name Paselli SA-6. The  $^1\text{H}$  NMR characterisation of the sample showed four doublets assigned to H-1 of reducing end groups in the  $\alpha$  and  $\beta$  configurations (at 5.27 and 4.58 ppm, respectively), the anomeric protons at (1  $\rightarrow$  6)-branch points (5.00 ppm), and the main signal at 5.40 ppm from the anomeric protons of (1  $\rightarrow$  4) linkages [12]. Integration of these resolvable resonances gave a dextrose equivalent (DE, the content of reducing end-groups relative to glucose as 100) of 4.3, which corresponds to a number-average molecular weight of 4100, and a degree of branching of 3.0%. Independent analysis of the same sample by gel permeation chromatography produced a DE value of 4.7 and a symmetrical curve in the molecular weight distribution (F. Deleyn, personal communication). The following slicing in molecular weight has been taken from the area observed by plotting the GPC signal intensity versus retention times:

MW	Area (%)
< 1000	6.71
$10^3$ – $5 \times 10^3$	21.26
$5 \times 10^3$ – $25 \times 10^3$	29.4
$25 \times 10^3$ – $2 \times 10^5$	39.76
$2 \times 10^5$ – $10^6$	2.87
$10^6$ – $5 \times 10^6$	0.01

A linear relationship was found to follow the development of gel strength as a function of concentration ( $C$ ) in SA-6 gels [14]:

$$\log G' = 8.28 \log C - 8.09 \quad (1)$$

where  $r^2 = 0.991$ ,  $G'$  is given in Pa, and the lowest detectable gelling concentration was ca. 10%.

*Methods.*—Gelatin samples were prepared by soaking the granules at room temperature overnight and then raising the temperature to 60 °C with gentle agitation. Maltodextrin samples were made by dissolving the powder at 90 °C for 15 min. Binary systems were produced by mixing appropriate amounts of the stock solutions at 70 °C. Mixed solutions were transferred immediately to the pre-heated cup (70 °C) of the Bohlin VOR rheometer, the bob was lowered, and the surface of the samples was covered with silicone fluid (50 cs) to prevent evaporation. The concentric cylinders defined a measuring geometry of 14-mm inner diameter and 15.3-mm outer diameter. The dynamic oscillation routine involved cooling the samples to 5 °C at a scan rate of 1 or 3 °C/min, and leaving them there for 7 h to approach asymptotically a constant value ('pseudoequilibrium' modulus). The flat dependence of modulus traces on oscillatory frequency (from 0.001 to 10 Hz), following the isothermal run at 5 °C, verified the development of permanent gels within the experimental constraints and allowed us to carry out temperature runs at the relatively high frequency of 1 Hz (0.2% strain). Finally samples were heated to 90 °C so that a complete picture of network gelation and melting was obtained. To enhance the understanding about the rates of different molecular processes in our mixture, extra rheological procedures were performed, namely, sample-setting at 20 or 25 °C for 7 h followed by controlled heating, and leaving the samples at 20 °C for 7 h but then cooling first to 5 °C and implementing another 7-h isothermal run before the concluding heating step.

The initial stages of phase separation were captured in the time–temperature continuum by monitoring the development of turbidity in samples using a Unicam SP8-100 spectrophotometer at the wavelength of 400 nm. Thus, mixed solutions were cooled from 70 to 5 °C at 1 °C/min and then left at 5 °C for 1 h, a routine which allowed recording of the extent of polymer demixing in the form of absorbance:  $A = \log(I_i/I_f)$ , where  $I_i$  and  $I_f$  are the incident and final intensities of the visible light at 400 nm. Finally, the microphase separation of gelatin and maltodextrin as a function of temperature was followed by microscopy. Mixed solutions were prepared at 70 °C and cooled to 10 °C in a water bath at a scan rate of 1 °C/min. At intervals of five degrees, samples were removed and frozen rapidly in liquid nitrogen. Pieces (10 × 10 × 3 mm) were cut from the solid material using a sharp scalpel. Each sample was stained with iodine

vapour and examined at a magnification of  $50\times$ . Images were acquired on TMax 100 photographic film using a Nikon inverted microscope Diaphot-TMD with bright field optics.

### 3. Results and discussion

*Pinpointing the phase inversion of the gelatin–maltodextrin system following its gelling and melting profiles.*—As mentioned in the introduction, earlier studies have shown that concentrated gelatin–maltodextrin systems phase-separate in solution at equilibrium [12], and that upon quench-cooling (it is ca.  $33\text{ }^{\circ}\text{C}/\text{min}$  in our setting) they form a composite gel with maltodextrin as the continuous phase penetrated by the gelatin filler [13]. Since the high rate of gelation might have ‘frozen’ the composite structure in a non-equilibrium arrangement, thus preventing the osmotic diffusion of solvent between phases, we decided to look at the physical properties of networks produced at lower cooling rates. Efforts were focused on the 5% gelatin series which allowed preparation of binary systems with a maltodextrin content up to 30%. As for the investigation of quench-formed gels, melting profiles of the control-cooled counterparts give a good idea of phase continuity in the mixtures.

Fig. 1a shows a typical heating run ( $1\text{ }^{\circ}\text{C}/\text{min}$ ) for samples within the 0–20% maltodextrin range. These have already been cooled from  $70$  to  $5\text{ }^{\circ}\text{C}$  at  $1\text{ }^{\circ}\text{C}/\text{min}$  and left there for 7 h to reach ‘pseudoequilibrium’ modulus. The pattern of structural collapse is identical to that of single gelatin gels, shown earlier for the quenched samples by Kasapis et al. [15], thus arguing for gelatin-continuous mixtures which liquefy early upon heating. As an index of melting temperature ( $t_{\text{mel}}$ ) we have used the frequency-dependent crossing of storage ( $G'$ ) and loss ( $G''$ ) moduli ( $t_{\text{mel}}$  is  $35\text{ }^{\circ}\text{C}$  for the 15% maltodextrin blend). Heating scans of samples at the second range of maltodextrin concentrations (from 22.5 to 30%) show entirely different behaviour, with structures weakening as the temperature rises, due to deconvolution of gelatin helices, but maintaining a dominant elastic response up to temperatures associated with melting of the maltodextrin network ( $t_{\text{mel}} > 65\text{ }^{\circ}\text{C}$ ) [15], thus creating a two-step heating profile (Fig. 1b).

Fig. 2a reproduces the trend in melting temperatures across the working range of maltodextrin concentrations. Clearly there is a sharp increase in the thermal stability of mixtures at maltodextrin concentrations between 20 and 22.5%, with the  $t_{\text{mel}}$  for the first group of data corresponding invariably to gelatin-continuous preparations. The second cluster of points, however, could indicate phase separation in the form either of a gelatin filler surrounded by a maltodextrin matrix (composite gel) or of a bicontinuous arrangement where both components form a continuous network. To uncover the true macromolecular organisation in the latter combinations, we had to consider the variation in the onset of gelation and define as  $t_{\text{gel}}$  the temperature at which  $G' = G''$  during cooling of the samples (frequency of 1 Hz). As shown in Fig. 2b, phase separation at maltodextrin concentrations between 10 and 20% has concentrated the gelatin phase, thus encouraging formation of a continuous gelatin matrix at higher temperatures ( $t_{\text{gel}}$  values rise progressively from ca. 20 to  $28\text{ }^{\circ}\text{C}$ ). There is a sharp drop in the pattern of

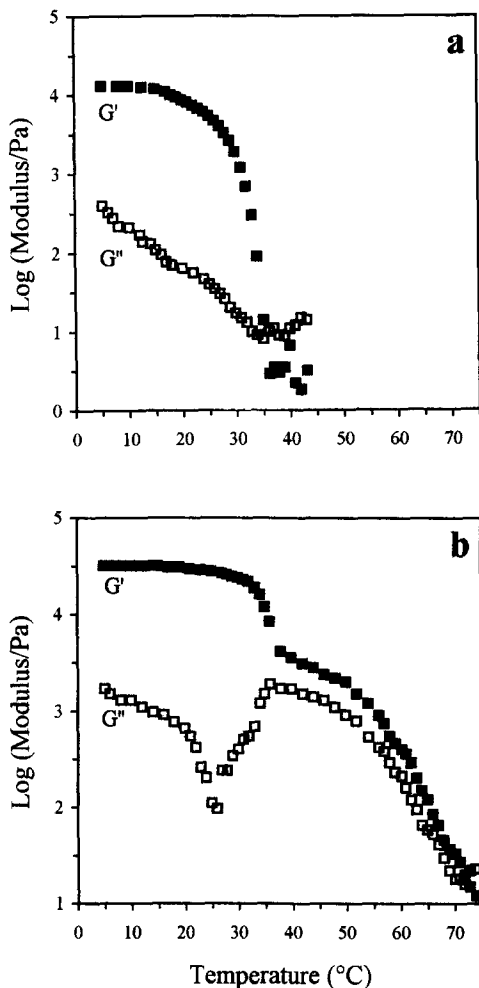


Fig. 1. Heating runs of (a) 5% LO-2 plus 15% SA-6 and (b) 5% LO-2 plus 27.5% SA-6 at a scan rate of 1 °C/min (frequency of 1 Hz; 0.2% strain).

$t_{\text{gel}}$  development at 22.5% maltodextrin ( $t_{\text{gel}} = 23$  °C), with the onset of gelation recovering at higher amounts of the polysaccharide. This should be the result of an increasingly concentrated maltodextrin phase which now forms the supporting matrix, since a continuous gelatin phase at higher concentrations of maltodextrin would follow the trend in  $t_{\text{gel}}$  observed at lower concentrations of the polysaccharide. Therefore the dramatic change in thermal properties signifies a true phase-inversion point from a gelatin- to a maltodextrin-continuous dispersion.

For the quenched samples, the visual estimation of the time required for the development of self-supporting networks at a fixed temperature was employed to show a steady reduction followed by a dramatic increase (phase-inversion point) and a final

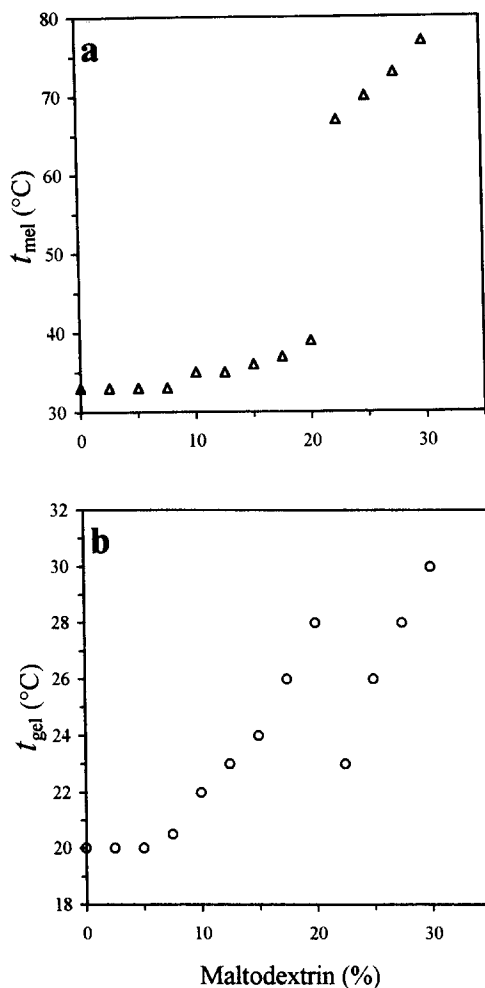


Fig. 2. Recording of the temperatures at which the  $G'$  and  $G''$  traces of the 5% LO-2 series cross over on (a) heating ( $t_{mel}$ ) and (b) cooling ( $t_{gel}$ ) at a scan rate of 1 °C/min (frequency of 1 Hz; 0.2% strain).

decrease as a function of increasing levels of maltodextrin (the gelatin concentration was kept constant) [15]. That was again rationalised in terms of the occurrence of phase transformation from a gelatin to a maltodextrin supporting matrix, but at a different polymer composition. This discrepancy in phase behaviour will be utilised to articulate much of the argument in the following section.

*Experimental evidence of kinetic influences on the state of phase separation in gelatin–maltodextrin gels.*—Fig. 3 summarises the effect of thermal regime on the gelation and phase separation of gelatin–maltodextrin solutions which were prepared at 70 °C. In the case of quench-cooling, there is a sharp increase in the values of storage modulus beyond 15% maltodextrin which is coincident with the phase inversion from gelatin- to maltodextrin-continuous composite gels. Below the phase-inversion point,

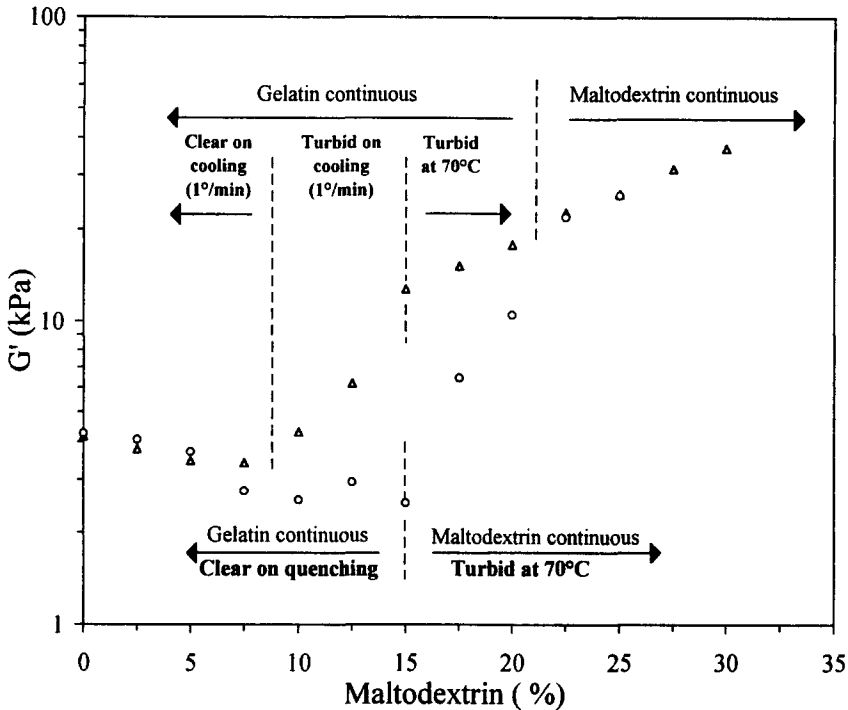


Fig. 3. Master curve for the development of storage modulus and turbidity in the 5% LO-2 series. Mixtures were either quenched (O) or scanned at 1 °C/min (Δ) from 70 to 5 °C and left there for 7 h, with the values of  $G'$  at the end of the isothermal run being plotted on the graph (frequency of 1 Hz; 0.2% strain).

mixed solutions remain clear, and upon gelation show a steady reduction in experimental moduli with increasing maltodextrin concentration, which was rationalised on the basis of gradually deswelled gelatin networks due to slow ordering of the polysaccharide [13]. For the maltodextrin-continuous combinations, however, samples become cloudy upon mixing at 70 °C and  $G'$  results were better described on the basis of immediate phase separation in solution and separate gelation of the two biopolymers.

In the event of controlled cooling at 1 °C/min, mixed preparations with a maltodextrin content up to 7.5% are clear during the cooling cycle (from 70 to 5 °C) and show the familiar reduction in moduli of deswelled gelatin networks. At combinations of 10 and 12.5% maltodextrin, samples are still clear at 70 °C but become turbid during controlled cooling, and there is an immediate reinforcing effect on the composite strength. Subsequent heating indicates gelatin-continuous mixtures since a gelatin-related heating profile is recorded (melting at ca. 35 °C in Fig. 2a). At maltodextrin concentrations from 15 to 20%, turbidity is observed upon mixing (70 °C) but there is no question that these gels (5 °C) are maltodextrin-continuous (like their quenched counterparts), since they also collapse at an early temperature during heating (for example, at 39 °C for the 20% SA-6 sample). At higher levels (from 22.5 to 30%), mixtures phase-invert to a maltodextrin supporting phase with a prolonged melting behaviour ( $t_{\text{mel}}$  is 67 and 77 °C, respectively, in Fig. 2a).



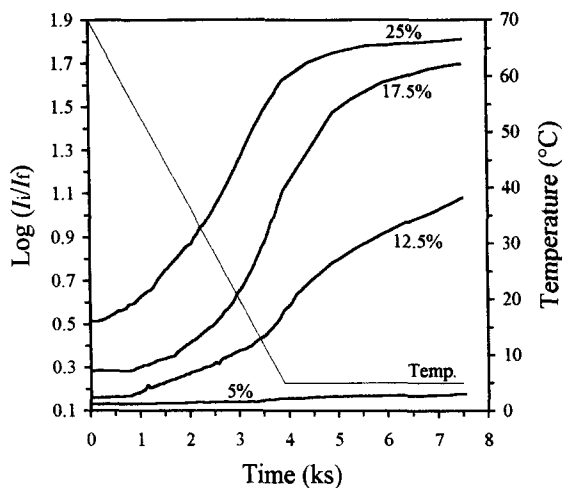


Fig. 4. Development of absorbance, monitored at the wavelength of 400 nm, for 5% LO-2 blends with levels of SA-6 shown by the individual traces. Samples were cooled from 70 to 5 °C at 1 °C/min and left there for 1 h.

As a convenient index, phase separation can be related to the pattern of storage modulus development if the absorbance,  $A = \log(I_i/I_f)$ , of mixtures is measured during cooling from 70 to 5 °C at the scan rate of the rheological work (1 °C/min). Readings were also taken at 5 °C for 60 min. Fig. 4 illustrates typical spectra of the response obtained for the experimental maltodextrin range, and Fig. 5 reproduces the measurements at the beginning ( $t = 0$  s) and the end ( $t = 3900$  s) of the cooling runs at 400 nm. Thus, clear preparations (up to 7.5% maltodextrin) produce absorbance values of 0.13

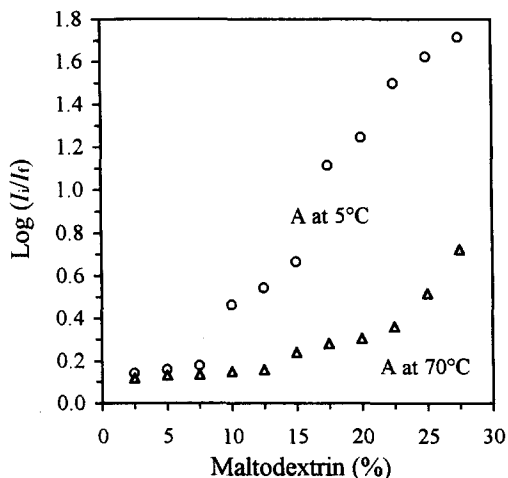


Fig. 5. Absorbance values of the gelatin–maltodextrin blends at the beginning (70 °C;  $t = 0$  s) and end (5 °C;  $t = 3900$  s) of cooling scans at 1 °C/min.

and 0.18 (Fig. 5), for example, for the 5% SA-6 sample at 70 and 5 °C, respectively, and convert into deswelled gelatin gels whose gelation temperature remains close to that observed for the single gelatin network in Fig. 2b. Vestiges of a phase-separated gel should appear at maltodextrin concentrations of 10 and 12.5% since the samples develop turbidity on scanning down, although they are still clear at 70 °C ( $A = 0.54$  and  $0.16$  for the 12.5% SA-6 combination at 5 and 70 °C, respectively; Fig. 5). Extensive phase separation is observed at maltodextrin concentrations between 15 and 20% with the opalescent preparations producing absorbance values of 0.28 and 1.12 at 70 and 5 °C, respectively (17.5% SA-6 sample in Fig. 5). The fourth and final category refers to phase-separated, maltodextrin-continuous systems which show significant turbidity throughout the experimental routine. For example, the composite of 25% maltodextrin produces absorbance values of 0.52 and 1.62 at 70 and 5 °C.

Considering the visual observations in combination with the evidence of Figs. 4 and 5, one can look back on Fig. 3 and propose that the system is under kinetic control. Obviously, the slower cooling makes the rate of phase separation faster than that of gelation so that steric exclusion in solution and subsequent gel reinforcement occur at maltodextrin concentrations as low as 10% in the mixture, whereas this is observed only beyond the phase-inversion point, occurring at ca. 15% maltodextrin, for the quenched samples. Furthermore, quenching of the cloudy, maltodextrin-continuous solutions at 17.5 and 20% polymer results in a maltodextrin-continuous composite gel, but for the same samples slow cooling allows sufficient time for the gelatin structure to develop and thus to phase-invert the mixture into gelatin-continuous gels.

Rheological evidence, however, is not sufficient to clarify the parentage of gelatin-continuous gels, produced by slow cooling (1 °C/min), at 10 and 12.5% SA-6 in the mixture. These preparations are clear at 70 °C but develop turbidity during cooling, which could be the result of a gelatin-continuous solution leading to a gelatin supporting matrix, or a maltodextrin-continuous solution with the low cooling rate inducing phase inversion to a protein-continuous gel at lower temperatures. As illustrated in the top micrograph of Fig. 6, samples become turbid at 60 °C and the maltodextrin-rich phase forms large streams with included areas of the gelatin-rich phase. At 30 °C the system is quite viscous and well-defined maltodextrin and gelatin areas are formed in what appears to be a bicontinuous solution. Further cooling of the mixture will gel the protein phase with the onset of network formation occurring at 23 °C, according to the empirical marker of Fig. 2b. Thus the bottom micrograph in Fig. 6 (taken at 20 °C) reproduces the three-dimensional structure of gelatin (white strands) supporting the liquid maltodextrin domains which show as dark, featureless images. As argued in the preceding paragraph, therefore, slow cooling of the 10% and 12.5% SA-6 mixed systems allows phase reversal to occur driven by the earlier gelation of the gelatin component.

*Using the kinetic approach to manipulate phase phenomena in the gelatin–maltodextrin composite gel.*—The profound consequences of thermal history on the viscoelastic properties of gelatin gels are well documented [16]. Differential scanning calorimetry work has shown that tempering of gelatin gels at temperatures between 15 and 30 °C before cooling to 5 °C yields networks with longer helices than those formed directly at 5 °C. The effect of thermal regime on gelatin gels was applied to our kinetic scheme in an attempt to extend the understanding and control further the phase behaviour of



Fig. 6. Bright-field-optics micrographs of 5% gelatin with 12% maltodextrin taken at 60, 30, and 20 °C (top, middle, and bottom images, respectively). In the top two micrographs, (\*) indicates the gelatin phase. Details of sample handling are given in the Methods part of the paper.

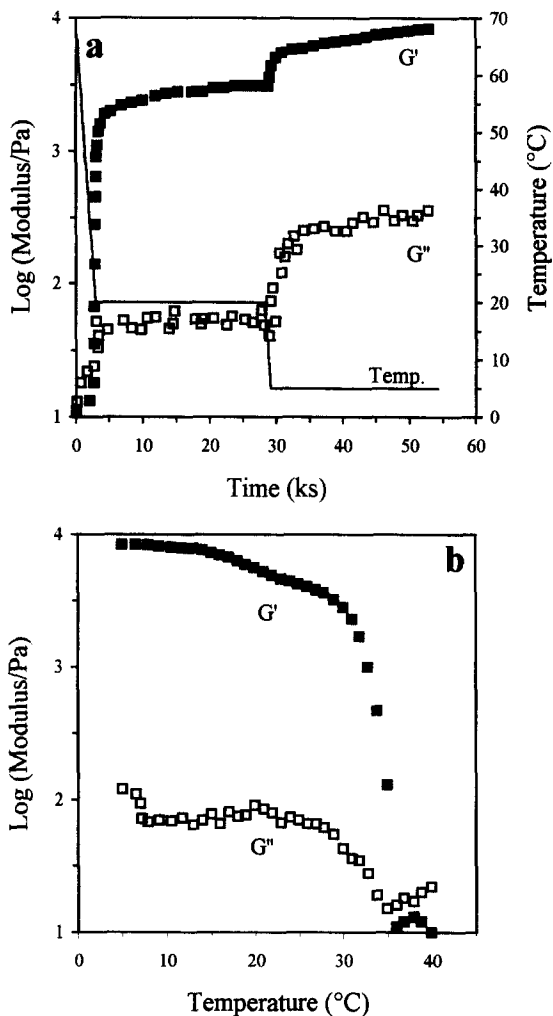


Fig. 7. Combined cooling-isothermal (a), and heating (b) runs for 5% LO-2 plus 12.5% SA-6 (frequency of 1 Hz; 0.2% strain).

gelatin–maltodextrin systems. Fig. 7a shows the gelling profile of a mixture (5% LO-2 plus 12.5% SA-6) that was cooled from 70 to 20 °C at 1 °C/min, left to set at 20 °C for 7 h, cooled at the end of the isothermal run from 20 to 5 °C (1 °C/min), and then allowed to develop ‘pseudoequilibrium’ modulus at 5 °C (7 h). Clearly two distinct ‘waves’ of structure were formed as a result of holding the sample at 20 and 5 °C. During subsequent heating in Fig. 7b, the temperature course of storage and loss moduli also shows a bimodal character (scan rate of 1 °C/min). The two-step melting profile is attributed to the initial melting of the shorter helices followed by the dissociation of the more thermally stable, longer helices which are formed mainly at 20 °C.

The selective formation of longer helices with increasing temperature creates more elastic gelatin networks which should be able to support higher amounts of the maltodextrin filler before the eventual transformation to a maltodextrin-continuous system. To demonstrate this, binary gels were made by cooling from 70 to 20 and 25 °C at a scan rate of 1 °C/min, holding the samples at the above temperatures for 7 h and finally heating back to record the melting profiles (1 °C/min). Observations were contrasted with the macromolecular characteristics of gels taken by cooling from 70 to 5 °C at 1 °C/min and holding there for 7 h, discussed already in Fig. 3. The heating scans of polymer compositions at which phase inversion occurs is reproduced in Fig. 8. At the three holding temperatures, changes in the storage modulus as a function of maltodextrin concentration are mapped out in Fig. 9. For each family of points illustrated, there is a clear transition from gelatin- to maltodextrin-continuous arrangements, which shifts from about 21 and 23.5 to 26% maltodextrin in Fig. 8 (temperatures of 5, 20, and 25 °C, respectively). For the holding temperatures of 20 and 25 °C, the phase inversion is also discernible in Fig. 9 since at this point the magnitude of storage modulus shows a discontinuity which is flanked by a steady increase in modulus over lower and higher ranges of maltodextrin concentration. Finally, one notices that the mixtures of 5% LO-2 with 25% SA-6 produce comparable network rigidities for the gels cured at 20 and 25 °C (maltodextrin- and gelatin-continuous gels, respectively). However, the two composites yield entirely different textural properties, the former being hard and brittle whereas the latter is rubbery and elastic. Clearly, there is a lot of potential for product development in this exercise, since thermal manipulation of maltodextrin–gelatin formulations can result in products as varied as confectioneries and low-fat pasties.

*Modelling of the kinetics of phase separation in the gelatin–maltodextrin gel.*—As discussed in Fig. 3, switching from fast cooling (quenching) to slow cooling at 1 °C/min slows down the process of molecular ordering and gelation, thus encouraging microscopic phase separation before the phase-inversion point. Cooling at an intermediate rate further demonstrates that the state of phase separation in mixed gels is under kinetic control. In Fig. 10, the values of storage modulus for the mixture of 5% LO-2 plus 15% SA-6, scanned from 70 to 5 °C at 3 °C/min, operate below those for the same preparation cooled at 1 °C/min (the development of  $G'$  was also monitored at 5 °C for 7 h). In both cases, the formation of a gelatin network at the beginning, setting up the supporting matrix, and the subsequent structuring of maltodextrin in the form of a discontinuous filler are captured in a time–temperature bimodal profile.

To characterise the relationship between network rigidity and phase phenomena in gelatin-continuous microstructures, we looked at the pattern of solvent partition between the two components since this would determine the effective polymer concentration and eventually the viscoelastic properties of a composite. In doing so, the experimental storage moduli of binary gels before the phase-inversion point, which were taken by scanning from 70 to 5 °C at 1 and 3 °C/min and leaving the samples there for 7 h, were used in Fig. 11 (for an explanation of this figure and of the computations involved see Appendix). For comparison, we have also included the points of quenched preparations showing deswelled gelatin gels (from 2.5 to 12.5% SA-6 plotted on the physically unrealistic maltodextrin-continuous bounds), and the phase-separated maltodextrin-con-

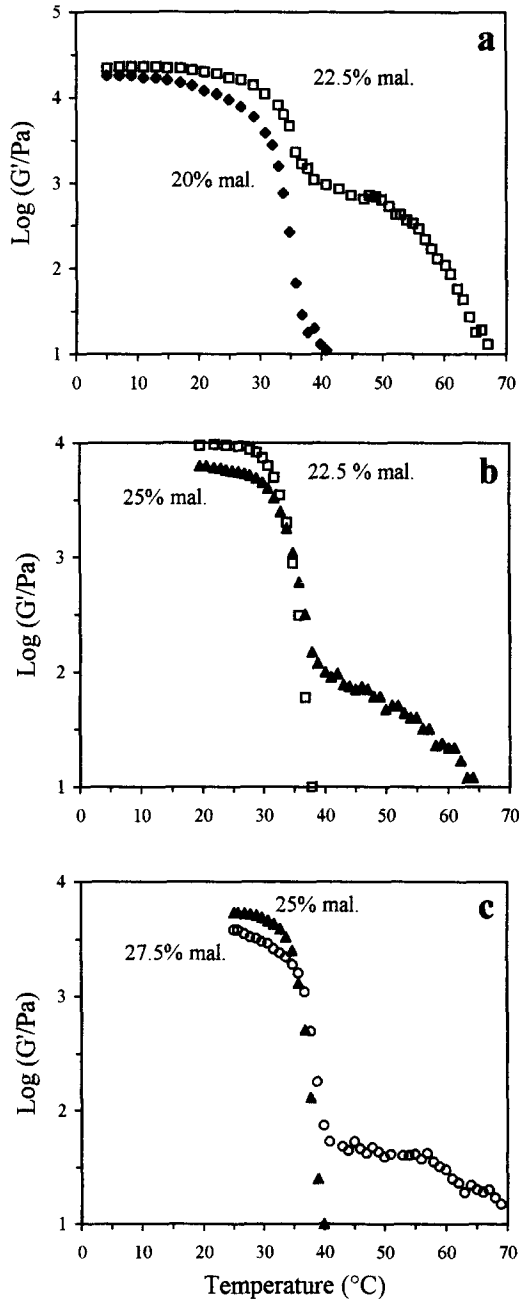


Fig. 8. Phase inversion from gelatin- to maltodextrin-continuous composite gels, as monitored by the melting profiles of storage modulus, for 5% LO-2 mixtures which were left at (a) 5, (b) 20, and (c) 25  $^{\circ}\text{C}$  for 7 h. The concentrations of SA-6 in the samples are shown by the mechanical spectra (heating at 1  $^{\circ}\text{C}/\text{min}$ ; frequency of 1 Hz; 0.2% strain).

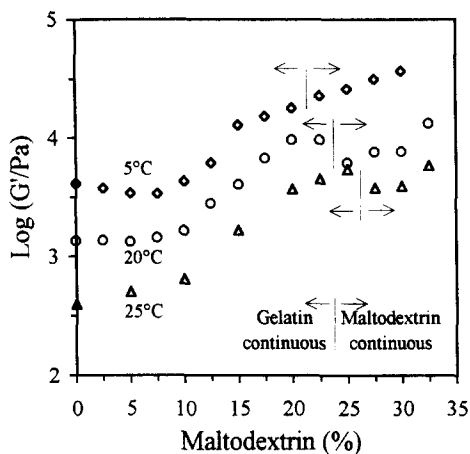


Fig. 9. Development of storage modulus as a function of maltodextrin concentration for the 5% gelatin blends which were cooled from 70 °C at 1 °C/min to 5 (◇), 20 (○), and 25 °C (△), and left there for 7 h (frequency of 1 Hz; 0.2% strain).

tinuous combinations at 15, 17.5 and 20% of the polysaccharide which intercept the corresponding physically realistic bounds.

In accordance with the visible spectrophotometry results (Figs. 4 and 5), samples cooled at 1 °C/min produce either deswelled gelatin gels (clear preparations up to 7.5% maltodextrin), or partially phase-separated arrangements for the blends of 10 and 12.5% maltodextrin which remain clear at a substantial part of the cooling run. The values of

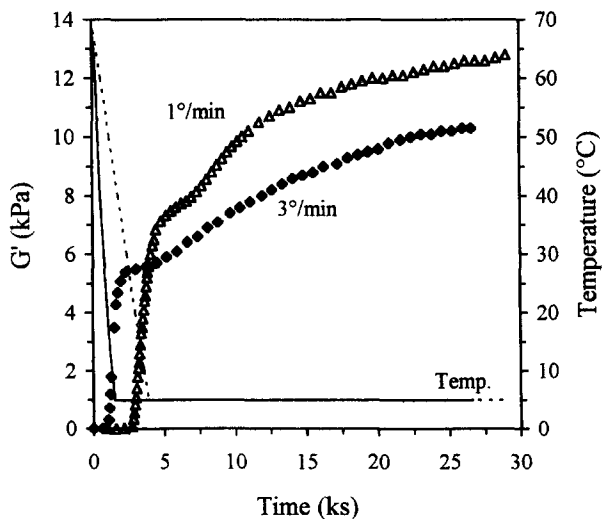


Fig. 10. Cooling of the 5% LO-2 plus 15% SA-6 mixture from 70 to 5 °C at 1 °C/min (---) and 3 °C/min (—). In both cases samples were left at 5 °C for 7 h.

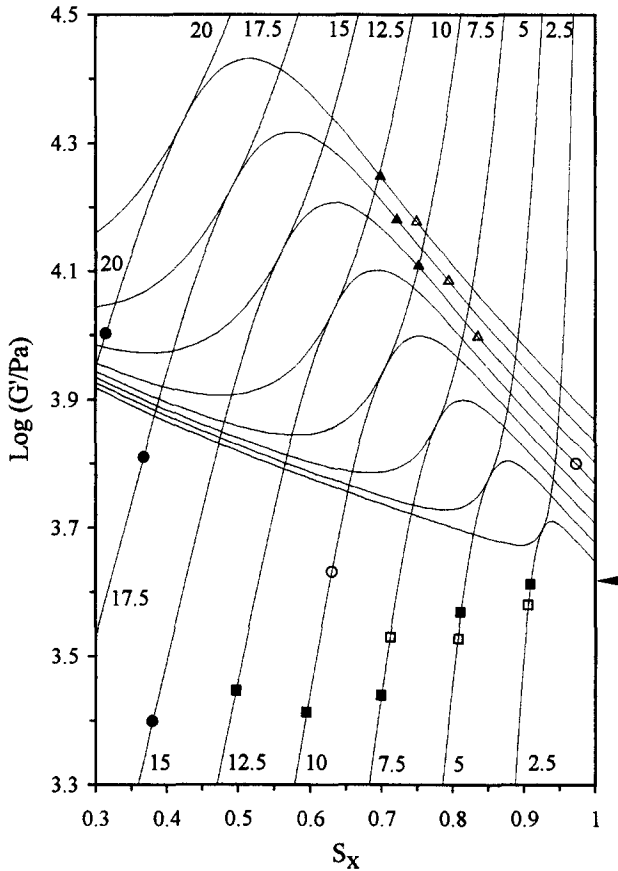


Fig. 11. Mixtures of 5% gelatin with increasing concentrations of maltodextrin by: quenching with deswelled LO-2 gels (■), and phase-separated maltodextrin-continuous arrangements (●); controlled cooling at 1 °C/min with deswelled gelatin gels (□), partially phase-separated gelatin-continuous gels (○), and completely phase-separated gelatin-continuous gels (▲); and controlled cooling at 3 °C/min with completely phase-separated LO-2-continuous gels (△). The network rigidity of a 5% gelatin gel is shown by the arrow on the right-hand axis.

storage modulus fall below, or in the case of 12.5% maltodextrin just manage to intercept, the gelatin-continuous bounds at unrealistically high values of gelatin solvent fraction ( $S_x = 0.975$  implying that almost all the solvent is in the gelatin phase, leaving effectively a dehydrated maltodextrin component). At higher concentrations of maltodextrin (15, 17.5, and 20%), solutions become turbid and phase-separate upon mixing at 70 °C, thus producing higher values of modulus for the gelatin-continuous gels at 5 °C which intercept the appropriate bounds. Extensive phase separation concentrates the gelatin phase and creates a sharp storage-modulus dependence as monitored by the cascade fit (see introduction); the gradient of  $G'$  growth tends to infinity at  $C_0$  and transforms to a linear dependence with a slope of ca. 2 at the concentrated regime [14]. However, the concentration dependence of storage modulus in clear solutions (up to



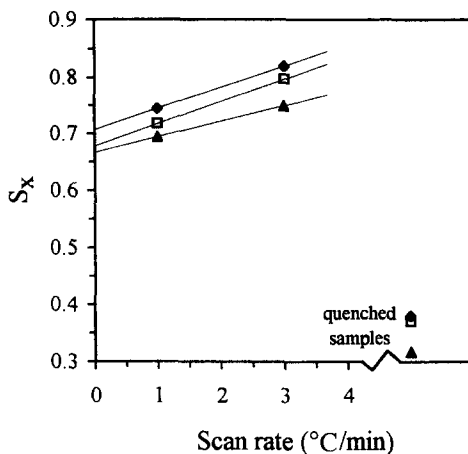


Fig. 12. Comparison of the solvent fraction in the gelatin phase for 15% (♦), 17.5% (□), and 20% (▲) SA-6 in the blend derived by extrapolation to zero scan rate with that taken from the quenched counterparts.

7.5% SA-6), which lead to deswelled gelatin arrangements at 5 °C, has been recorded to follow the lower value of  $q = 0.667$  (deswelling factor) [13].

Following the kinetic argument of Fig. 10, the last three combinations (15, 17.5 and 20% SA-6) were scanned at 3 °C/min and it was found that they intercept the gelatin-continuous bounds at lower  $G'$  values than for the 1 °C/min counterparts (Fig. 11). Similarly, the magnitude of storage modulus for the 2.5–12.5% SA-6 preparations cooled at 3 °C/min falls below the corresponding values of the 1 °C/min samples, thus failing to intercept the gelatin-continuous bounds (not shown in Fig. 11 to avoid clutter). Therefore greater cooling rates (ranging from 1 °C/min to quenching) accelerate ordering and aggregation during cooling, thus increasingly freezing the system in a microstructure that bears parentage to the arrangement in solution and slowing down the redistribution of solvent between phases.

To eliminate the effect of cooling rates on the solvent fraction of constituent phases with 15, 17.5, and 20% maltodextrin, the corresponding values of  $S_x$  were extracted from Fig. 11 and plotted as a function of scan rate in Fig. 12. The solvent fractions of the gelatin phase at zero scan rate (i.e., allowing infinite time for equilibration between the cascading thermal steps) were found to be 0.708, 0.678, and 0.664 for the 15, 17.5, and 20% maltodextrin blends, respectively. The variation in solvent fraction of the gelatin phase with maltodextrin concentration was recast in the form of relative solvent partition between the two constituent polymers, using the following formula [9]:

$$p = (S_x/x)/([1 - S_x]/y) \quad (2)$$

where  $x$  is the original (nominal) concentration of gelatin (5%) and  $y$  denotes the corresponding concentrations of SA-6 (15, 17.5, and 20%). A straightforward calculation yields a constant  $p$  value of  $7.6 \pm 0.3$  in favour of the gelatin component. Quenched combinations in the foregoing SA-6 range have already phase-inverted in maltodextrin-continuous arrangements (see Fig. 3), thus producing a distinct family of

points in Fig. 11 ( $S_x$  values have been taken from Fig. 11). The solvent fraction of gelatin in these gels lies between 0.317 and 0.380, a result which produces a  $p$  value of  $1.8 \pm 0.2$ . Clearly, there is a dramatic change in the distribution of solvent between the two phases as a result of varying the thermal regime whereby gelatin holds 760% more solvent than the polysaccharide per unit concentration when it forms the supporting matrix whereas this excess is reduced to only 80% in the maltodextrin-continuous gels. Therefore, the polymer that forms the continuous matrix holds a disproportionate amount of solvent in its phase. The solvent tries to diffuse in the anisotropic medium in an attempt to establish osmotic equilibrium, but it seems that, within the experimental time–temperature constraints, gels are kinetically trapped away from conditions of thermodynamic equilibrium.

In conclusion, both the experimental observations and the quantitative treatment provide a general outline for the analysis of phase phenomena in binary biopolymer gels. In our view, dominant kinetic influences in the gelatin–maltodextrin system make prediction of structure formation in composite gels from phase diagrams in solution at equilibrium quite doubtful. Instead, the development of network rigidity and in general the composite viscoelasticity, the polymer composition at which phase inversion occurs, and the relative solvent partition between two phases will be governed heavily by the operational temperature course.

## Acknowledgements

The authors are pleased to acknowledge stimulating discussions with their colleagues on the ‘Behaviour of Biopolymer Mixtures in Structuring Food Products’ MAFF-DTI Link project, Mr A. Parker (Systems Bio-Industries, France) for providing analytical data of the gelatin sample, and Dr F. Deleyn (Cerestar, Belgium) for communication of unpublished results.

## Appendix

To explore the distribution of solvent between the gelatin and maltodextrin phases, we calculate values of  $G'$  for all possible distributions, and find those which match the experimental values. Gelatin is denoted as polymer X and maltodextrin as polymer Y. Solvent partition is defined by  $S_x$ , the fraction of the water present in the gelatin phase. At very low concentrations of polymer,  $S_x$  and  $(1 - S_x)$  are virtually identical to the phase volumes  $\phi_x$  and  $(1 - \phi_x)$ . At the wide range of concentrations used in the present work the values diverge due to direct contribution of macromolecules to phase volume at higher concentrations of polymer. To establish a relationship between solvent fraction and phase volume, the concentration-dependence of gel density was monitored by filling a pre-weighed measuring cylinder with the appropriate solution, allowing the gel to form, reading off its volume, and determining its relative density from the ratio of the weight of the gel to the weight of the same volume of water. Values for gelatin and

maltodextrin lie on straight lines, yielding the following relationship between polymer concentration ( $C$ ) and relative density ( $D$ ) for each phase:

$$D_x = 1.0 + RC_x, \quad D_y = 1.0 + RC_y \quad (3)$$

with the slope of the line giving a numerical value of  $R = 0.0034$ . Then, for a particular combination of the two polymers (e.g., 5% LO-2 plus 17.5% SA-6), the total weight of a phase ( $tw_x$  or  $tw_y$ ) is the sum of polymer weight ( $x$  or  $y$ ) and water ( $w_x$  or  $w_y$ ) in each phase. For each possible distribution of the total weight of water ( $w$ ) between the component phases of the above mixture (values of solvent fraction,  $S_x$ , vary from 0 to 1 at steps of 0.01 in the computerised algorithm) the water in the phases and the total weight of the phases are:

$$w_x = S_x w, \quad w_y = (1 - S_x) w, \quad (4)$$

$$tw_x = x + w_x, \quad tw_y = y + w_y. \quad (5)$$

The effective concentrations (% w/w) of gelatin and maltodextrin in their respective phases are given by:

$$C_x = 100x/tw_x, \quad C_y = 100y/tw_y, \quad (6)$$

and the relative volumes of the two phases can be estimated by the corresponding ratios of  $tw$  and  $D$ :

$$V_x = tw_x/D_x, \quad V_y = tw_y/D_y. \quad (7)$$

At the end, phase volumes in the composite system are given in terms of the relative volumes of regions X and Y as follows:

$$\phi_x = V_x/(V_x + V_y), \quad 1 - \phi_x = V_y/(V_x + V_y). \quad (8)$$

Therefore knowing the starting (nominal) concentrations of X and Y, the final (effective) concentrations in the individual phases can be calculated, which in turn give the moduli  $G_x$  and  $G_y$  of the two phases from experimental calibration curves in the way described for gelatin (cascade fit) and maltodextrin (linear relationship) in the Experimental section. The analysis assumes that gelation results in pure gelatin- or maltodextrin-continuous phases, or in other words the binodal of a phase diagram in solution shifts close to the co-ordinate axes during formation of a phase-separated gel. The overall modulus of the composite gels can then be calculated by the isostrain and isostress blending laws in the numerical form laid out by Takayanagi et al. [10]:

$$G_U = \phi_x G_x + (1 - \phi_x) G_y, \quad (9)$$

$$1/G_L = \phi_x/G_x + (1 - \phi_x)/G_y. \quad (10)$$

For  $G_x > G_y$  and the polymer X forming the supporting matrix, the above approach gives an isostrain or upper bound behaviour ( $G_U$  in Eq. 9) whereas phase inversion in the system, with the polymer X being now the discontinuous filler, results in the so-called isostress or lower bound model ( $G_L$  in Eq. 10).

Fig. 13 reproduces schematically the computerised output of a phase-separated gelatin–maltodextrin combination (e.g., 5% LO-2 plus 17.5% SA-6) plotted against the

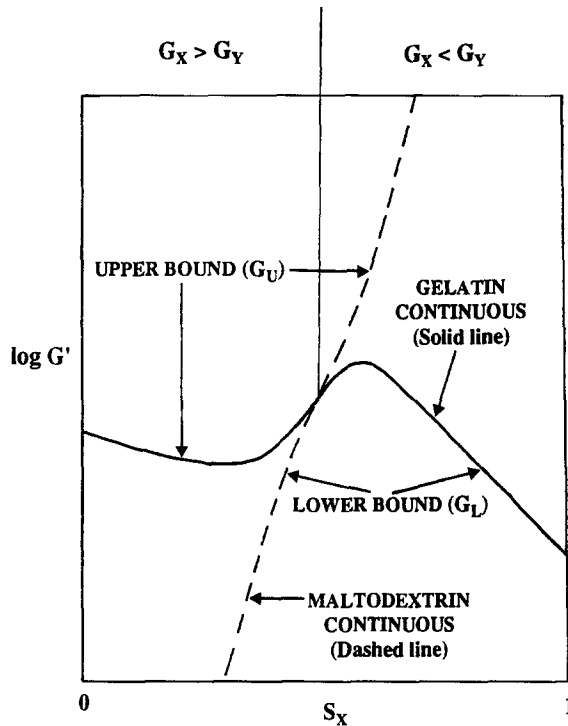


Fig. 13. Schematic variation of calculated moduli as a function of solvent fraction in the LO-2 phase for a composite gelatin–maltodextrin gel.

solvent fraction in the gelatin phase. At very low values of  $S_x$ , where most of the water is in the maltodextrin phase, the gelatin is extremely concentrated, and thus  $G_x \gg G_y$ . Conversely, at very high values of  $S_x$ ,  $G_x \ll G_y$ . At one critical value of  $S_x$ , the moduli of the two phases cross over (with  $G_x = G_y = G_U = G_L$ ). Up to this point, the upper bound value of ( $G_U$ ) corresponds to a gelatin-continuous system and the lower bound value ( $G_L$ ) to a maltodextrin-continuous system. At higher values of  $S_x$ ,  $G_U$  relates to a maltodextrin-continuous system and  $G_L$  to a gelatin-continuous system.

## References

- [1] A.A. McKinnon, D.A. Rees, and F.B. Williamson, *Chem. Commun.*, (1969) 701–702.
- [2] N.S. Anderson, J.W. Campbell, M.M. Harding, D.A. Rees, and J.W.B. Samuel, *J. Mol. Biol.*, 45 (1969) 85–99.
- [3] D.A. Rees, *Biochem. J.*, 126 (1972) 257–273.
- [4] G.T. Grant, E.R. Morris, D.A. Rees, P.J.C. Smith, and D. Thom, *FEBS Lett.*, 32 (1973) 195–198.
- [5] Yu.A. Antonov, V.Ya. Grinberg, and V.B. Tolstoguzov, *Stärke*, 27 (1975) 424–429.
- [6] V.Ya. Grinberg and V.B. Tolstoguzov, *Carbohydr. Res.*, 25 (1972) 313–321.
- [7] Yu.A. Antonov, V.Ya. Grinberg, and V.B. Tolstoguzov, *Colloid Polym. Sci.*, 255 (1977) 937–947.

- [8] Yu.A. Antonov, N.V. Losinskaya, V.Ya. Grinberg, V.T. Dianova, and V.B. Tolstoguzov, *Colloid Polym. Sci.*, 257 (1979) 1159–1171.
- [9] A.H. Clark, R.K. Richardson, S.B. Ross-Murphy, and J.M. Stubbs, *Macromolecules*, 16 (1983) 1367–1374.
- [10] M. Takayanagi, H. Harima, and Y. Iwata, *Mem. Fac. Eng. Kyushu Univ.*, 23 (1963) 1–13.
- [11] F.W. Cain, A.H. Clark, P.J. Dunphy, M.G. Jones, I.T. Norton, and S.B. Ross-Murphy, Eur. Patent, 0298 561 (1989).
- [12] S. Kasapis, E.R. Morris, I.T. Norton, and M.J. Gidley, *Carbohydr. Polym.*, 21 (1993) 249–259.
- [13] S. Kasapis, E.R. Morris, I.T. Norton, and A.H. Clark, *Carbohydr. Polym.*, 21 (1993) 269–276.
- [14] S. Kasapis, E.R. Morris, I.T. Norton, and A.H. Clark, *Carbohydr. Polym.*, 21 (1993) 243–248.
- [15] S. Kasapis, E.R. Morris, I.T. Norton, and C.R.T. Brown, *Carbohydr. Polym.*, 21 (1993) 261–268.
- [16] J.P. Busnel, S.M. Clegg, and E.R. Morris, *Melting Behaviour of Gelatin Gels: Origin and Control*, in G.O. Phillips, P.A. Williams, and D.J. Wedlock (Eds.), *Gums and Stabilisers for the Food Industry 4*, IRL Press, Oxford, 1988, pp 1–11.